Chinese Chemical Letters 33 (2022) 2512–2516

Contents lists available at ScienceDirect

Chinese Chemical Letters

journal homepage: www.elsevier.com/locate/cclet

Nanobody-based polyvinyl alcohol beads as antifouling adsorbents for selective removal of tumor necrosis factor-α

Lichun Wang[a], Yu Ding[b], Nan Li[a], Yamin Chai[a], Qiyu Li[b], Yunzheng Du[a], Zhangyong Hong[b,*], Lailiang Ou[a,*]

[a] The key Laboratory of Bioactive Materials, Ministry of Education, College of Life Sciences, Nankai University, Tianjin 300071, China
[b] State Key Laboratory of Medicinal Chemical Biology, Tianjin Key Laboratory of Protein Sciences, College of Life Sciences, Nankai University, Tianjin 300071, China

ARTICLE INFO

Article history:
Received 12 July 2021
Revised 27 December 2021
Accepted 31 December 2021
Available online 7 January 2022

Keywords:
Nanobody
Polyvinyl alcohol beads
Immunosorbents
Tumor necrosis factor-α
Adsorption

ABSTRACT

Highly efficient removal of tumor necrosis factor-α (TNF-α) from plasma by hemoperfusion for autoimmune disease therapy remains a challenge in the clinical field owing to the low adsorption capacity and poor blood compatibility of adsorbents. In this work, a new class of nanobody (Nb)-coupled antifouling polyvinyl alcohol (PVA) beads was constructed as an immunosorbent for the selective removal of TNF-α from plasma. Notably, our immunosorbent exhibited an exceptionally high specific TNF-α adsorption capacity of 416.9 ng/g in human plasma (at a plasma-to-adsorbent ratio of 300). More importantly, the obtained adsorbent beads showed outstanding blood compatibility. In addition, during *in vivo* experiments, the blood circulation device was constructed to remove TNF-α in rat models, proving that the beads had good removal performance (~85%/60 min). Furthermore, 95% of the original capacity was retained after 6-month storage, showed strong stability and prolonged storage of PVA-Nb. Above all, the results indicate that the novel PVA-Nb immunosorbent has possible clinical applications for treating autoimmune diseases in the clinic.

TNF-α, a crucial immunomodulatory cytokine produced by macrophages, plays vital roles in inflammation, antitumor responses, and infections [1]. However, it is a double-edged sword [2]. It can eliminate pathogens and promote tissue repair, but as the primary cytokine in inflammation, it accelerates the outburst of other cytokines and induces cytokine release syndrome (or a cytokine storm), which can exacerbate the inflammatory state and lead to immune dysfunction [3]. Clinically, one fifth of corona virus disease 2019 (COVID-19) cases have been found to progress to severe illness, septic shock, and multiple organ failure owing to this cytokine storm [4]. In addition, elevated levels of TNF-α in blood are associated with many human diseases, including sepsis, chronic hepatitis B, autoimmune diseases (such as inflammatory bowel disease and rheumatoid arthritis [RA]), insulin resistance and tumorigenesis [5]. Thus, eliminating aberrant TNF-α from blood plasma has become a major focus in the treatment of the aforementioned ailments, including COVID-19 [6]. Three FDA-approved therapeutic agents (adalimumab, infliximab, and etanercept) are effective for treating RA and other autoimmune diseases [7]. However, all of them have obvious shortfalls: They are costly and associated with side effects, including neurological disorders and heart failure [8]. Fortunately, hemoperfusion is an effective and economical technology that can inhibit TNF-α [9–11]. One commercial extracorporeal hemoperfusion device, the CytoSorb^{TM} adsorber (CytoSorbents Corporation, Monmouth Junction, NJ, USA) [12], has been successfully employed to rebalance the immune system and moderate cytokine storms as an adjunctive therapy for patients with COVID-19. CytoSorb^{TM} can remove a substantial proportion of most cytokines both *in vivo* and *in vitro*. However, it can only remove 20%–30% of the trimeric form of TNF-α, which is the largest cytokine (at 51 kDa) [13,14]. To address this, a wide variety of porous adsorbents have been crosslinked with anti-TNF-α antibodies and antibody fragments, and have shown exceedingly high selectivity and efficiency for the elimination of TNF-α [15,16]. DiLeo *et al.* fabricated an anti-TNF-α hemoperfusion device combining CytoSorb^{TM} with TNF-α antibodies, which significantly enhanced the adsorption ability of TNF-α [17]. Indeed, antibodies are employed as ligands with high specificity and strong binding affinity in hemoperfusion, however, poor stability and the high cost of antibodies are the major limitations to their further application in immunosorbent therapy, especially for hemoperfusion [18–21]. Therefore, in-

* Corresponding authors.
E-mail addresses: hongzy@nankai.edu.cn (Z. Hong), ouyll@nankai.edu.cn (L. Ou).

https://doi.org/10.1016/j.cclet.2021.12.087
1001-8417/

troducing more stable, cost-effective, and efficient ligands will undoubtedly lead to a more effective solution.

Scientists in Belgium discovered interesting heavy-chain-only antibodies (HCAbs) in camels; these contain a variable domain of heavy chain HCAbs (VHHs) and two conventional CH_2 and CH_3 regions [22]. More importantly, as the smallest unit binding target antigen, VHH, known as the single domain antibody or nanobody (Nb), can be cloned independently and easily, and has shown exceptional structural stability and antigen-binding activity [23]. Nb can be used in different formats such as monovalent, bivalent, and polyvalent. Among them, bivalent Nbs are coming to the forefront of therapeutic applications owing to their outstanding affinities and potencies [24]. The unique biophysical and biochemical properties of bivalent Nbs make them ideally suited as ligands for hemoperfusion immunosorbents [25].

Polyvinyl alcohol (PVA) beads have been investigated as an ideal carrier owing to their outstanding mechanical properties, sufficient mesoporous structure, and fantastic biocompatibility, which are vital for hemoperfusion. Furthermore, a large number of hydroxyl groups exist in PVA, which can easily be functionalized *via* noncovalent and covalent chemical interactions. In addition, PVA beads are antifouling polymers with few adverse effects on blood components.

In this study, we developed Nb-coupled antifouling polyvinyl alcohol beads as immunosorbents. Our *in vitro* study showed that the TNF-α level could be restored to a normal level within 10 min of the experiment. An extracorporeal blood circulation device was constructed to remove TNF-α in rat models, further proving that the beads had good removal performance (~85%/60 min). Furthermore, 95% of the original capacity was retained after 6-month storage, which showed outstanding stability of PVA-Nb. These results provide critical insight into how fabricate nanobody beads for hemoperfusion and their potential for the removal of TNF-α from plasma.

To construct the beads, bivalent anti-TNF-α Nb was expressed overnight at 30 °C using the pPICZαA vector in *Pichia pastoris* cells and purified *via* nickel-ion affinity chromatography. Amino acid sequence, production, and purification details are provided in the experimental section of Support information, while the characterization of Nb is shown in Fig. S1 (Supporting information). A yield of 100 mg Nb per liter culture was acquired and the bivalent Nb was analyzed *via* sodium dodecyl sulfate-polyacrylamide gel electrophoresis (SDS-PAGE) (Fig. S1a). The results of enzyme-linked immunosorbent assays (ELISA) indicate the excellent binding capacity of Nb to TNF-α, with a K_D value of 4.36 nmol/L (Fig. S1b). According to matrix-assisted laser desorption/ionization time of flight mass spectrometry (MALDI-TOF MS) technology, the molecular weight of the Nb was 28,026.95 Da (Fig. S1c).

As shown in Fig. 1a and Fig. S2 (Supporting information), covalent immobilization of Nb on the PVA beads depends on the reactive epoxy groups. The degree of epoxidation was detected by acid-base titration, and the epoxy value of PVA was 120–130 μmol/g wet matter, which fulfilled the immobilization requirements.

To investigate the morphologies of the constructed beads, a stereo microscope was used. Stereo microscope images of a few particles from both PVA and PVA-Nb revealed that the macroscopical morphology of beads was spherical with a diameter of around 75–120 μm (Fig. S3 in Supporting information). A closer examination of the scanning electron microscope (SEM, Figs. 1b–e) showed spherical absorbents with a well-developed porous structure. This indicates that epoxidation and Nb immobilization did not affect the porous structure, as clear mesopores could still be seen on their rough external surfaces.

The chemical structure and elements of PVA and PVA-Nb were characterized *via* Fourier transform infrared (FT-IR) spectroscopy (Fig. 1f) and X-ray photoelectron spectroscopy (XPS) analyses (Figs. 1g-i and Table S1 in Supporting information), respectively. After the functionalization with Nb, the PVA peak at 1086 cm^{-1} had shifted to 1069 cm^{-1}, probably due to the overlapping of the Nb peak at 1058 cm^{-1} (the existence of methionine). This indicates that Nb was present in the PVA-Nb beads (more details are provided in the results and discussion section of Supporting information). Sulfur is a characteristic element of Nb in the PVA-Nb beads. XPS was conducted to investigate the chemical composition of PVA, in which the C, N and O elements are present. In the C 1s spectrum of PVA (Fig. 1g), three deconvoluted peaks centered at 284.6, 285.9, and 289.2 eV could be assigned to C–C, C–N and C=O, respectively [26]. The presence of C–N and C=O in PVA could be attributed to the functional groups in the crosslinker. It is also noteworthy that no sulfur was detected. Regarding PVA-Nb, C, N, O and S elements were observed. In the C 1s spectrum of PVA-Nb (Fig. 1h), three deconvoluted peaks located at 284.6, 286.1 and 289.1 eV could also be assigned to C-C, C-N and C=O bonds. However, one new peak was found at 287.7 eV, and this was assigned to the C-S bond [27]. The presence of that bond confirms the existence of S as well as the successful conjugation of Nb. Fig. 1i shows the S 2p spectrum of PVA-Nb. There were two deconvoluted peaks centered at 163.6 and 164.4 eV, which were assigned to the S-H and S-C bonds, respectively [28]. The presence of these bonds is in good accordance with the functional groups in the Nb. These results again confirm that the Nb was successfully integrated into the sample. Moreover, the content of S determined by XPS was 0.08 at%.

We also conducted fluorescence labeling to provide more direct evidence of the existence of Nb on PVA-Nb beads. Nb was labeled with fluorescein isothiocyanate (FITC). Fig. S4 (Supporting information) shows the images of FITC-Nb immobilized PVA compared with unmodified PVA beads. An obvious fluorescence signal is observed for the PVA-Nb but not the initial PVA beads. These data confirm the presence of Nb on the PVA-Nb beads.

In order to further understand the amount of Nb grafting on PVA, a BCA protein assay and a western blotting assay (Fig. S5 in Supporting information) were conducted. The amount of Nb immobilized on the carrier was determined by the difference between the amount of Nb in the solution before fixation and the amount of Nb in the eluent after fixation. From the BCA protein assay, the graft rate of Nb was as high as 63.59% (Fig. S5d). The result was also obtained in the western blotting assay (67.84% grafting rate) (Fig. S5c).

Next, we investigated their adsorption performance using human plasma with high TNF-α concentrations (approximately 1000 pg/mL), in accordance with the levels in sepsis patients [29]. To this end, we performed adsorption experiments, including assessments of time-dependent adsorption kinetics, plasma/adsorption ratios, adsorption isotherms, the effect of temperature, the preservation stability, and specific adsorption ability (Fig. 2 and Figs. S7-S10 in Supporting information). PVA beads were used in control experiments. As depicted in Fig. 2a and Fig. S7, the uptake of TNF-α by PVA-Nb is quite rapid and reaches equilibrium within 10 min, which can be explained by Nbs designed to remove TNF-α. The final TNF-α adsorption rate of PVA-Nb reached 99.75%, with an adsorption capacity of 46.98 ng/g. By contrast, PVA alone had rates of only 13.93% and 6.20 ng/g, respectively. Next, we analyzed the adsorption kinetics of TNF-α at 37 °C onto three adsorbents (PVA, PVA-Nb, and CYT (a commercial adsorbent, USA)) using two extensively used kinetic models (*pseudo*-first-order and *pseudo*-second-order models) [30]. The equations used for nonlinear fitting, the relevant parameters ($Q_{e,exp}$, $Q_{e,calc}$, k), and the correlation coefficients (R^2) are provided in the experimental section and Table S3 (Supporting information). Both models had high R^2 values (greater than 0.995). This suggests that whether hydrophobic and electrostatic action played an important role in the adsorp-

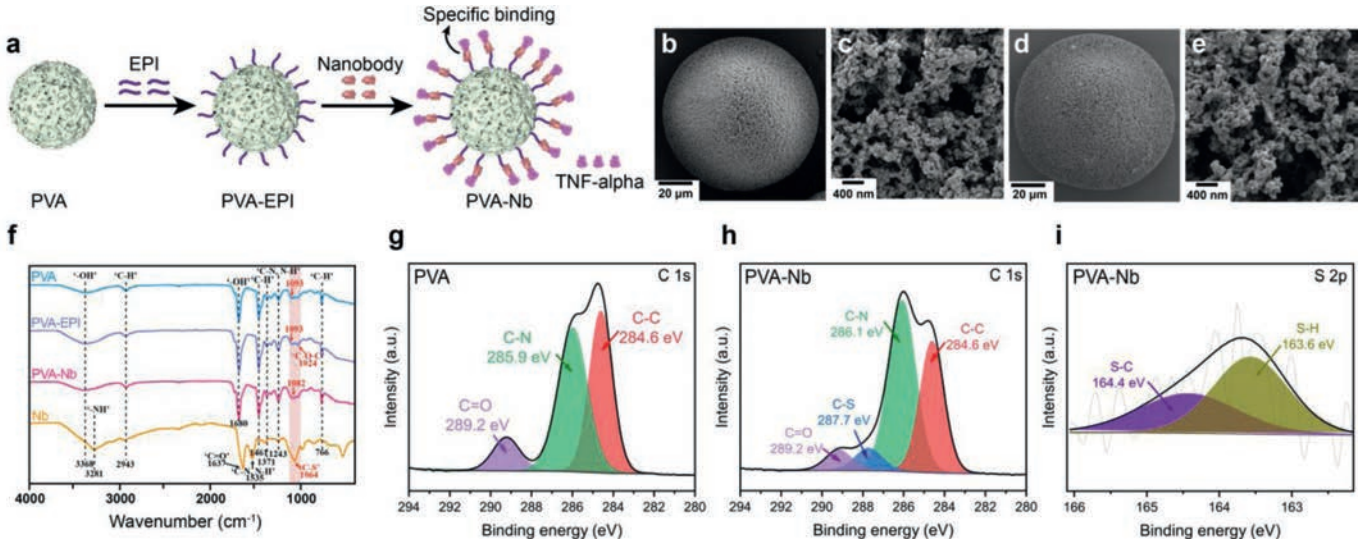

Fig. 1. (a) Scheme of the PVA-Nb microspheres prepared by two reactions (substitute and opening-ring reaction) of epichlorohydrin (EPI). SEM micrographs of PVA (b, c) and PVA-Nb beads (d, e). (f) FT-IR spectra of PVA, PVA-EPI, PVA-Nb beads and Nb. (g) XPS C 1s high-resolution spectra of PVA. XPS C 1s (h) and S 2p (i) high-resolution spectra of PVA-Nb.

tion of TNF-α by PVA-Nb beads. However, the R^2 value of *pseudo*-second-order model fit the experimental data better, with a much higher R^2 value. Interestingly, the equilibrium adsorption capacities of the *pseudo*-second-order model ($Q_{e,calc}$) were much closer to the experimental values ($Q_{e,exp}$), indicating that electrostatic action played the most vital role. To better mimic a fever *in vivo* condition, time-dependent adsorption kinetics at 42 °C were conducted (Fig. S8 and Table S4 in Supporting information). The uptake of TNF-α by PVA-Nb at 42 °C was also quite rapid and reached equilibrium within 10 min. The results are quite similar to those at 37 °C, which met the requirements of practical applications for hemoperfusion (the detailed discussion is provided in Supporting information). The plasma/adsorption ratios assay (Fig. S9a) indicated that the adsorption rate of TNF-α remained high (93.80%), with an adsorption capacity of 416.9 ng/g, at a volume ratio of plasma-to-resin of 300, owing to the high affinity of PVA-Nb for TNF-α. As shown in Fig. S9b, the adsorption isotherm for TNF-α of PVA-Nb is classified as the S-1 type, according to Giles's method. The adsorption of TNF-α increased slowly when the equilibrium TNF-α concentration in plasma was lower owing to the competitive adsorption of other protein components in human plasma and increased quickly when a certain concentration range had been reached. This is because of the interaction between the free and adsorbed TNF-α factors in plasma [2]. With the rapid improvement of the adsorption rate and binding capacity, PVA-Nb became more efficient than the commercial CYT. Regarding temperature effects (Fig. 2b), PVA-Nb exhibited remarkable TNF-α uptake values of 98.1% ± 2.02%, 98.07% ± 1.01%, 99.52% ± 0.36%, 98.47% ± 1.23% and 98.82% ± 0.24% at 8, 21, 37, 42, and 45 °C, respectively, while PVA had much lower rates of 0.42% ± 0.35%, 0.48% ± 0.22%, 12.94% ± 1.00%, 3.12% ± 0.36% and 0.90% ± 0.41%, respectively. It is obvious that TNF-α uptake did not change much as the temperature increased, probably owing to the stability and specificity of the Nb-based immunosorbent. An ideal immunosorbent for clinical applications should be robust enough to allow prolonged storage in an economical and practical way. To test this, PVA-Nb beads were stored in normal saline for 6 months, and adsorption capacity was assessed each month. The beads maintained an extremely similar adsorption rate (greater than 95%) throughout the time period (Fig. 2c), confirming its excellent preservation stability, and indicating that it is a more practical TNF-α adsorbent than other immunosorbents. To further examine the specificity of PVA-Nb, the beads were loaded with human plasma supplemented with several major plasma proteins, such as TNF-α, IL-1β, IL-2 and IL-6, whose concentrations before and after adsorption were measured *via* ELISA. As shown in Fig. S10 (Supporting information), the material adsorbs TNF-α with a high selectivity and without nonspecific adsorption to a variety of other blood components. It also showed excellent TNF-α selectivity in the hyperinflammatory plasma from a rat model of sepsis (Fig. 2d). In addition, it had better adsorption than blank PVA beads and CYT beads. To further test the blood-cleaning capability of PVA-Nb beads *in vivo*, we conducted dynamic hemoperfusion experiments in rats with sepsis (Fig. 2e). The use of experimental animals was approved by the Animal Experiments Ethical Committee of Nankai University and the experiments were carried out in conformity with the Guide for Care and Use of Laboratory Animals. As we observed in our *in vitro* studies, the hemoperfusion device obtained significantly ($P < 0.0001$) low levels of TNF-α from the septic rat's blood within 1 h using PVA-Nb beads than those in infected animals treated with hemoperfusion either in the absence of added beads or using PVA beads (Fig. 2f). Moreover, hemoperfusion using PVA-Nb beads did not affect the composition of blood, including white blood cells (WBC), red blood cells (RBC), hemoglobin (HGB), and platelet (PLT) (Fig. S11 in Supporting information). Finally, all of these results are consistent with the *in vitro* experiments using human plasma. Taken together, these results imply that the PVA-Nb beads provide an excellent mesoporous structure with unexpectedly high stability and an enhanced adsorption rate and target–binding capacity, making them a more efficient TNF-α adsorbent than the CYT beads.

To assess the blood compatibility of the PVA-Nb beads and PVA beads, hemolysis experiments, routine blood tests, and coagulation assays were conducted [31]. In the hemolysis assay, the hemolysis ratio for PVA-Nb beads was 0.26% ± 0.11% (< 5%), indicating that the functionalization of Nb on the PVA beads exhibited little risk of facilitating hemolysis during application (Fig. S12 in Supporting information). The influence of PVA-Nb beads on blood components after 60 min of direct contact is depicted in Fig. 3a. The beads had negligible negative effects on the majority of blood cells including WBC, RBC, HGB, and PLT compared to the normal group. The blood coagulation properties of PVA-Nb beads were further assessed using four clinical assays, including assessments of prothrombin time

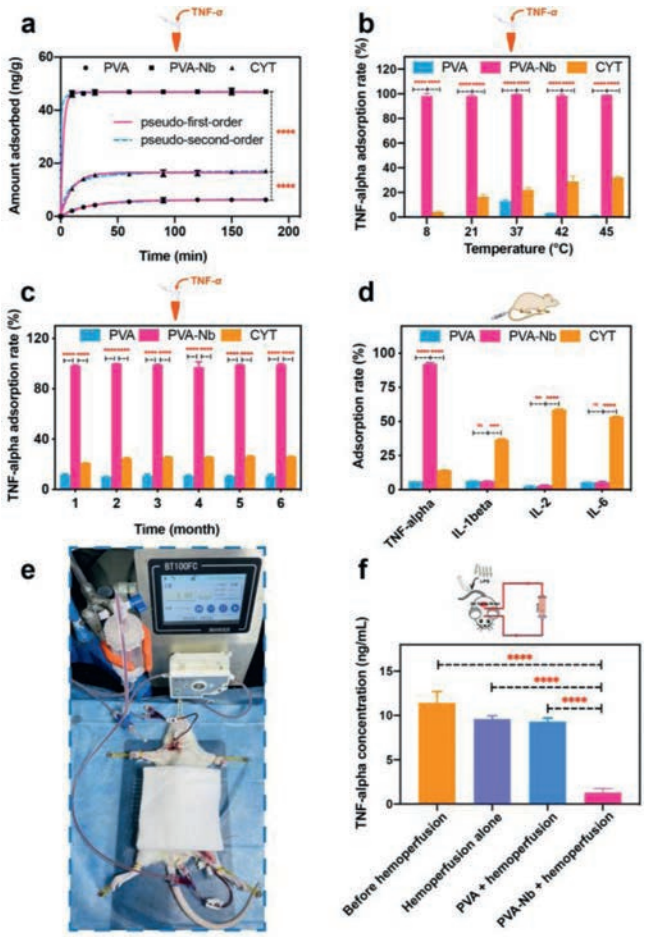

Fig. 2. Adsorption characteristics of PVA-Nb in the plasma of human and rat models of sepsis. (a) Non-linear fitting of the adsorption kinetics of TNF-α onto the three adsorbents in human plasma (T = 37 °C, $C_{TNF\text{-}\alpha}$ = 1417.19 ± 1.32 pg/mL). (b) Effects of temperature on the adsorption of TNF-α (t = 2 h, $C_{TNF\text{-}\alpha}$ = 873.47 ± 1.18 pg/mL). (c) Stability of PVA-Nb (T = 37 °C). (d) *In vitro* study of the adsorption performance of PVA-Nb beads in plasma from a rat model of sepsis (t = 2 h, $C_{TNF\text{-}\alpha}$ = 10.295 ± 0.28 ng/mL; $C_{IL\text{-}1\beta}$ = 1508.75 ± 0.38 pg/mL; $C_{IL\text{-}2}$ = 1231.18 ± 0.14 pg/mL; $C_{IL\text{-}6}$ = 143.429 ± 0.29 ng/mL). The plasma-to-adsorbent ratio is 20 in all the above experiments, and all values are expressed as mean ± SD (n = 3). (e) Photograph of the experimental animal setup for extracorporeal hemoperfusion. (f) Depletion of TNF-α levels for the entire 1-h treatment period in a sepsis rat model (n = 5). ns: not significant, $^{**}P < 0.01$, $^{***}P < 0.001$, $^{****}P < 0.0001$.

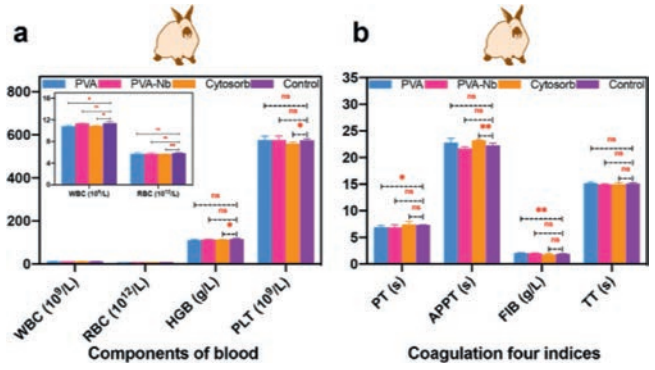

Fig. 3. Blood compatibility of the PVA and PVA-Nb beads. (a) Routine blood assays after 60 min of contact with adsorbents. (b) Coagulation assays of adsorbents (mean ± SD, n = 3). ns: not significant, $^{*}P < 0.05$, $^{**}P < 0.01$.

(PT), the activated partial thromboplastin time (APTT), thrombin time (TT), and fibrinogen (FIB) levels [32]. Compared to the control, PVA-Nb beads did not show any significant changes in PT, APTT, TT, or FIB levels (Fig. 3b), indicating their good anticoagulant properties. Altogether, these results demonstrate that the PVA-Nb has perfect blood compatibility.

In conclusion, we prepared a TNF-α selective immunosorbent for hemoperfusion after covalent immobilization of anti-TNF-α Nb. PVA-Nb beads exhibited biocompatible properties including low hemolysis rates (< 1%), negligible changes in blood components, and reasonable effects on blood coagulation properties. In tests on human plasma, the beads achieved an ideal adsorption capacity of 416.9 ng/g (when the plasma-to-adsorbent ratio was 300). In addition, experiments using hyperinflammatory plasma from a rat model of sepsis confirmed the selective removal of TNF-α without a significant reduction in other blood proteins. During *in vivo* studies, the hemoperfusion device was constructed to remove TNF-α in rat models, further proving that the beads had good removal performance (~85%/60 min). Moreover, the adsorption performance did not change with an increase in temperature from 8 °C to 45 °C, indicating strong stability. In addition, the material was storable, as in tests, 95% of the original capacity was retained after 6-month storage. Therefore, PVA-Nb beads may have great potential for clinical application for efficient and safe TNF-α adsorption from blood. They may inhibit cytokine storms and thus improve the clinical outcomes of patients with sepsis and various inflammatory diseases.

Declaration of competing interest

The authors declare that they have no known competing financial interests or personal relationships that could have appeared to influence the work reported in this paper.

Acknowledgments

This study was supported by grants from the National Key R&D Program of China (No. 2017YFC1104401), the National Natural Science Foundation of China (No. 81771986), the Natural Science Foundation of Tianjin (No. 18YFZCSY00860), and the Scientific Research Translational Foundation of Wenzhou Safety (Emergency) Institute of Tianjin University (No. TJUWYY2022004).

Supplementary materials

Supplementary material associated with this article can be found, in the online version, at doi:10.1016/j.cclet.2021.12.087.

References

[1] X.M. Zhou, Z.B. Zheng, H.Y. Liu, et al., Chin. Chem. Lett. 18 (2007) 905–908.
[2] G. Cheng, Y. Chai, J. Chen, et al., Chem. Commun. 53 (2017) 7744–7747.
[3] H. Li, L. Liu, D. Zhang, et al., The Lancet 395 (2020) 1517–1520.
[4] C. Huang, Y. Wang, X. Li, et al., The Lancet 395 (2020) 497–506.
[5] B.B. Aggarwal, Nat. Rev. Immunol. 3 (2003) 745–756.
[6] W. Sun, Y. Wu, M. Zheng, et al., J. Med. Chem. 63 (2020) 8146–8156.
[7] J.D. Lewis, New Engl. J. Med. 357 (2007) 296–298.
[8] T.T. Hansel, H. Kropshofer, T. Singer, et al., Nat. Rev. Drug Discov. 9 (2010) 325–338.
[9] J.H. Kang, M. Super, C.W. Yung, et al., Nat. Med. 20 (2014) 1211–1216.
[10] S. Shen, F. Han, A. Yuan, et al., Biomaterials 189 (2019) 60–68.
[11] C. Shi, X. Wang, L. Wang, et al., Nat. Commun. 11 (2020) 1–13.
[12] T. Eichhorn, S. Rauscher, C. Hammer, et al., Inflammation 39 (2016) 1737–1746.
[13] C. Tripisciano, O.P. Kozynchenko, I. Linsberger, et al., Biomacromolecules 12 (2011) 3733–3740.
[14] S. Yachamaneni, G. Yushin, S.H. Yeon, et al., Biomaterials 31 (2010) 4789–4794.
[15] C. Völlenkle, S. Weigert, N. Ilk, et al., Appl. Environ. Microbiol. 70 (2004) 1514–1521.
[16] V. Weber, I. Linsberger, M. Ettenauer, et al., Biomacromolecules 6 (2005) 1864–1870.
[17] M.V. DiLeo, J.D. Fisher, B.M. Burton, et al., J. Biomed. Mater. Res. B: Appl. Biomater. 96B (2011) 127–133.

[18] J. Chen, J. Sun, W. Han, et al., J. Mater. Chem. B 6 (2018) 4368–4379.
[19] A.M. Bossi, Nat. Chem. 12 (2020) 111–112.
[20] T.W. Kang, I.J. Hwang, S. Lee, et al., Adv. Mater. 33 (2021) 2101376.
[21] J. Xu, H. Miao, J. Wang, et al., Small 16 (2020) 1906644.
[22] C. McMahon, A.S. Baier, R. Pascolutti, et al., Nat. Struct. Mol. Biol. 25 (2018) 289–296.
[23] C. Hamers-Casterman, T. Atarhouch, S. Muyldermans, et al., Nature 363 (1993) 446–448.
[24] R.M. Awad, Q. Lecocq, K. Zeven, et al., Mol. Ther.-Meth. Clin. D 22 (2021) 172–182.
[25] C. Huang, J. Ren, F. Ji, et al., Acta Biomater. 107 (2020) 232–241.
[26] Y. Liu, Y. Zhao, Y. Jia, et al., Chem. Eng. J. 424 (2021) 130303.
[27] Z. Zhou, P. Zhao, C. Wang, et al., Microchim. Acta 187 (2020) 1–9.
[28] S.M. Li, Y.S. Wang, S.T. Hsiao, et al., J. Mater. Chem. C 3 (2015) 9444–9453.
[29] J. Cohen, E. Abraham, J. Infect. Dis. 180 (1999) 116–121.
[30] W. Zhu, X. Huang, Y. Zhang, et al., Chin. Chem. Lett. 32 (2021) 3382–3386.
[31] Y.J. Wang, Y.T. Yu, Artif. Cell. Blood Sub. 39 (2011) 92–97.
[32] N.D. Paul, T. Krämer, J.E. McGrady, et al., Chem. Commun. 46 (2010) 7124–7126.